



## Anthracene-terpyridine metal complexes as new G-quadruplex DNA binders



Sofia Gama <sup>a,\*</sup>, Inês Rodrigues <sup>a</sup>, Filipa Mendes <sup>a</sup>, Isabel C. Santos <sup>a</sup>, Elisabetta Gabano <sup>b</sup>, Beata Klejevskaja <sup>c</sup>, Jorge Gonzalez-Garcia <sup>c</sup>, Mauro Ravera <sup>b</sup>, Ramon Vilar <sup>c</sup>, António Paulo <sup>a</sup>

<sup>a</sup> Centro de Ciências e Tecnologias Nucleares (C<sup>2</sup>TN), Instituto Superior Técnico, Universidade de Lisboa, Portugal

<sup>b</sup> Dipartimento di Scienze e Innovazione Tecnologica, Università del Piemonte Orientale "Amedeo Avogadro", Alessandria, Italy

<sup>c</sup> Department of Chemistry, Imperial College London, London SW7 2AZ, UK

### ARTICLE INFO

#### Article history:

Received 2 November 2015

Received in revised form 15 March 2016

Accepted 3 April 2016

Available online 9 April 2016

#### Keywords:

G-quadruplex  
Terpyridine derivatives  
Platinum complexes  
Copper complexes  
DNA interaction  
c-myc

### ABSTRACT

The formation of quadruple-stranded DNA induced by planar metal complexes has particular interest in the development of novel anticancer drugs. This is especially relevant for the inhibition of telomerase, which plays an essential role in cancer cell immortalization and is overexpressed in ca. 85–90% of cancer cells. Moreover, G-quadruplexes also exist in other locations in the human genome, namely oncogene promoter regions, and it has been hypothesized that they play a regulatory role in gene transcription. Herein we report a series of new anthracene-containing terpyridine ligands and the corresponding Cu(II) and Pt(II) complexes, with different linkers between the anthracenyl moiety and the terpyridine chelating unit. The interaction of these ligands and metal complexes with different topologies of DNA was studied by several biophysical techniques. The Pt(II) and Cu(II) complexes tested showed affinity for quadruplex-forming sequences with a good selectivity over duplex DNA. Importantly, the free ligands do not have significant affinity for any of the DNA sequences used, which shows that the presence of the metal is essential for high affinity (and selectivity). This effect is more evident in the case of the Pt(II) complexes. Moreover, the presence of a longer linker between the chelating terpyridine unit and the anthracene moiety enhances the interaction with G-quadruplex-forming sequences. We further evaluated the ability of the Cu(II) complexes to interact with, and stabilize G-quadruplex containing regions in oncogene promoters via a polymerase stop assay. These studies indicated that the metal complexes are able to induce G-quadruplex formation and stop polymerase activity.

© 2016 Elsevier Inc. All rights reserved.

### 1. Introduction

G-quadruplex DNA is a thermodynamically stable topology of DNA which has been proposed to be functionally relevant to a number of essential biological processes. In particular, it has been suggested that quadruplexes play a role in regulation of gene expression, translation, telomere-end maintenance, recombination and replication [1–5]. Therefore, G-quadruplexes have emerged as novel and distinctive targets for the development of anticancer drugs [6,7]. G-quadruplexes are four-stranded DNA structures formed from stacked tetrads of hydrogen-bonded guanine bases. These stable, non-classical, secondary structures are formed in vitro at physiological salt concentration and pH, from DNA sequences containing stretches of adjacent guanine residues [8,9]. There is mounting experimental evidence indicating that these non-canonical DNA structures are also present in vivo [10–12]. Interestingly, stabilization of intramolecular telomeric DNA in a G-quadruplex conformation has been shown to inhibit its elongation

by the enzyme telomerase [4]. As telomerase is expressed in most cancer cells at substantially higher levels than in normal somatic cells, the enzyme is a potentially attractive target for selective anti-cancer therapy and drug development [13]. Telomerase itself is not an oncogene, but its repression and tight regulation in humans can be a tumour suppressor, and its targeting has advantages such as relative universality and specificity for cancer cells [14–18].

In addition to telomeric DNA, an intramolecular-quadruplex forming sequence has also been identified in the promoter region of the *c-myc* oncogene, amongst other gene promoters [6], and stabilization of this quadruplex structure has been implicated in the downregulation of the transcription of the gene [19,20]. All these facts suggest that a deeper understanding of quadruplex recognition by synthetic molecules could provide the basis of a novel anticancer drug.

Thus, researchers have taken up the challenge of synthesizing ligands that stabilize the quadruplex folded conformation focusing on the fact that a desired molecule should bind a human G-quadruplex structure with high affinity and with specificity over duplex DNA [21–23]. The number of known G-quadruplex ligands has increased steadily and several classes of quadruplex-targeting ligands have been reported that selectively bind to and stabilize quadruplexes [24–30]. Many of these ligands present a large planar aromatic surface, cationic

\* Corresponding author.

E-mail address: [sofia.gama@uni-jena.de](mailto:sofia.gama@uni-jena.de) (S. Gama).

<sup>1</sup> Current address: Institute für Anorganische und Analytische Chemie, Friedrich-Schiller-Universität Jena, Germany.

charges, and ability to adopt a terminal stacking mode [22,23]. In this context, the use of metal complexes as G-quadruplex binders is becoming very attractive due to the often easier synthetic access and their promising DNA binding properties [22]. The cationic or highly polarized nature of metal complexes is expected to promote the association with the negatively charged G-quadruplex-DNA [22,23]. Therefore, this approach assumes that the central metal centre can be positioned over the cationic channel of the quadruplex, optimizing the stacking interactions of the surrounding chelating agent with the accessible G-quartet. For instance, it has been reported that some Schiff base metal complexes are highly effective stabilizers of the human telomeric DNA, in particular square planar complexes of copper(II) and nickel(II) that are very prone to stack with the G-quartet [31–33]. Other types of ligands, namely derived from porphyrins and terpyridines, have been also tested and the corresponding Cu(II) and Pt(II) complexes were shown to act as G-quadruplex binders with high affinity and selectivity [34].

One of the features that quadruplex DNA binders should have if they are to be leads in drug discovery, is high selectivity over duplex DNA to minimise potential side effects. A successful strategy to improve such selectivity relies on the use of structures containing more than one interlinked planar polyaromatic moieties (e.g. anthracene, naphthalene, bipyridine or pyrene). As reported by Teulade-Fichou et al. [35], this type of strategy was successfully applied for macrocyclic organic compounds of the bis-intercalator or tris-intercalator type. This success inspired us to explore a similar approach to improve the quadruplex-selectivity of M(II)-terpyridine (M = Cu, Pt) complexes, known to interact with G-quadruplex sequences [34,36–40], by combining these terpyridine metal cores with a planar intercalating anthracenyl group.

Herein we report on the synthesis of a series of new anthracene-containing terpyridine ligands and the corresponding Cu(II) and Pt(II) complexes (Scheme 1) and on the biophysical characterization of their interaction with DNA of different topologies. In this work, the terpyridine chelating unit and the anthracenyl moiety were assembled using linker chains with different length and polarity, as we had anticipated that the different structural motifs (metal geometry, linker and pendant DNA intercalator) could influence the selectivity of the compounds' interaction with quadruplex DNA over duplex DNA. The interactions between ligands and metal complexes with the different topologies of DNA were studied by a variety of biophysical and spectroscopic techniques including FRET melting assays, fluorescence and CD spectroscopy. A polymerase stop assay was also performed to assess

the ability of the compounds to interact and stabilize G-quadruplex containing regions in an oncogene promoter.

## 2. Experimental section

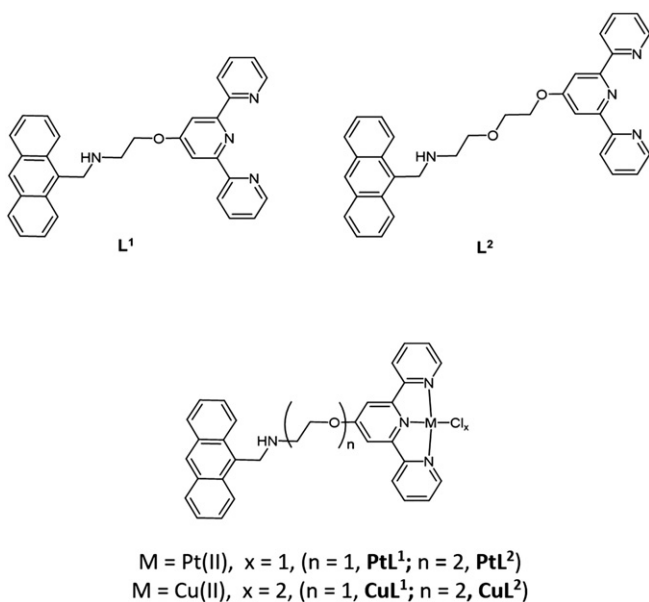
All chemicals used were analytical grade and used as received. The chemical reactions were followed by thin-layer chromatography (TLC), which was performed on precoated silica plates 60 F<sub>254</sub> (Merck). Visualization of the plates was carried out using Ultraviolet (UV) light (254 nm). Gravity column chromatography was carried out on silica gel (Merck, 70–230 mesh). The multinuclear NMR spectra were measured on a Bruker 500 MHz nuclear magnetic resonance (NMR) Spectrometer at 500 MHz (<sup>1</sup>H), 100.5 MHz (<sup>13</sup>C), and 85.9 MHz (<sup>195</sup>Pt), or in a Varian Unity 300 MHz spectrometer, and chemical shifts are given in ppm, referenced with the residual solvent resonances relative to SiMe<sub>4</sub>. <sup>1</sup>H and <sup>13</sup>C NMR chemical shifts were reported in parts per million referenced to solvent resonances. <sup>195</sup>Pt NMR spectra were recorded using a solution of K<sub>2</sub>[PtCl<sub>4</sub>] in saturated aqueous KCl as external reference. The shift for K<sub>2</sub>[PtCl<sub>4</sub>] was adjusted to –1628 ppm relative to Na<sub>2</sub>[PtCl<sub>6</sub>] (δ = 0 ppm). For the Pt(II) complexes, Reversed Phase-High-performance liquid chromatography (RP-HPLC) and mass analysis were performed using a Waters LC-MS (Liquid chromatography-mass spectrometry) instrument equipped with Alliance 2695 separations module, 2487 dual lambda absorbance detector, and 3100 mass detector. Electrospray ionisation mass spectrometry (ESI-MS) was performed with a Micromass ZMD mass spectrometer (Micromass, Manchester, UK). Typically, a diluted solution of the compound in methanol (with 2% of the suitable co-solvent) was delivered directly to the spectrometer source at 0.01 mL min<sup>-1</sup> by Hamilton microsyringe controlled by a single-syringe infusion pump. The nebulizer tip operated at 3000–3500 V and 150 °C, with nitrogen used both as a drying and a nebulizing gas. The cone voltage was usually 30 V. For the chelators and Pt(II) complexes, ESI-MS was performed on a QITMS (Quadrupole ion trap mass spectrometry) instrument in positive and negative ionisation mode. Peaks were assigned on the basis of the *m/z* values and of the simulated isotope distribution patterns. Elemental analysis (EA) was performed on an EA 110 CE Instruments automatic analyzer.

### 2.1. Synthesis

#### 2.1.1. Synthesis of 2-([2.2':6',2''-terpyridin]-4'-yloxy)-N-(anthracen-9-ylmethyl)ethan-1-amine (**AntTerp**, **L**<sup>1</sup>)

To a solution of anthracene-9-carbaldehyde (2.062 g; 10 mmol) in a 25% CH<sub>3</sub>OH/CH<sub>2</sub>Cl<sub>2</sub> solution (10 mL) 2-aminoethanol (0.72 mL, 12 mmol) was added. The reaction mixture was let to react overnight, at room temperature and under N<sub>2</sub>. After vacuum removal of solvent, the solid residue was redissolved in 50% CH<sub>3</sub>OH/CH<sub>2</sub>Cl<sub>2</sub> solution (20 mL) and NaBH<sub>4</sub> (1.1349 g, 30 mmol) was added, at 0 °C. After 18 h reaction at room temperature, the solvent was removed and the residue dissolved in CH<sub>2</sub>Cl<sub>2</sub> (50 mL) and washed with a solution of Na<sub>2</sub>CO<sub>3</sub> (pH 10, 3 × 50 mL). The organic layer was dried over Na<sub>2</sub>SO<sub>4</sub> and the solvent removed under vacuum to obtain 2-(anthracen-9-ylmethylamino)ethanol (**1**, **AntOH**). Yield: 2.238 g (89%). <sup>1</sup>H NMR (CDCl<sub>3</sub>-d<sub>3</sub>) δ: 8.42 (1H, s, H<sub>28</sub>), 8.32 (2H, d, H<sub>23</sub> + <sub>33</sub>), 8.01 (2H, d, H<sub>26</sub> + <sub>30</sub>), 7.51 (4H, ddt, H<sub>25</sub> + <sub>24</sub>, H<sub>31</sub> + <sub>32</sub>), 4.75 (2H, d, H<sub>20</sub>), 3.70 (2H, td, H<sub>16</sub>), 3.2 (2H, m, H<sub>19</sub>), 2.17 (1H, s, NH) ppm.

Then, 2-(anthracen-9-ylmethylamino)ethanol (0.251 g, 1 mmol) was let to react with 4'-chloro-2.2':6',2''-terpyridine (0.250 g, 0.9 mmol) and KOH (0.281 g, 5 mmol) in dimethyl sulfoxide (DMSO) for 4 h at 60 °C. The reaction was extracted with CH<sub>2</sub>Cl<sub>2</sub> (3 × 40 mL) and the organic layer washed with water (3 × 30 mL). The organic layer was dried over Na<sub>2</sub>SO<sub>4</sub> and the solvent was removed under vacuum. The solid residue was purified by column chromatography (100% CH<sub>2</sub>Cl<sub>2</sub> to 95/5 CH<sub>2</sub>Cl<sub>2</sub>/CH<sub>3</sub>OH) to afford 2-([2.2':6',2''-terpyridin]-4'-yloxy)-N-(anthracen-9-ylmethyl)ethan-1-amine (**AntTerp**, **L**<sup>1</sup>), which



**Scheme 1.** Structural formulae of the new anthracene-containing terpyridine ligands (**L**<sup>1</sup> and **L**<sup>2</sup>) and the corresponding Cu(II) and Pt(II) complexes (**CuL**<sup>1</sup>, **CuL**<sup>2</sup>, **PtL**<sup>1</sup> and **PtL**<sup>2</sup>).

was recovered as a pale brownish solid after removal of the solvent from the collected fractions. Yield: 205 mg (48%). ESI-MS ( $\text{CH}_3\text{OH}$ ): ( $m/z$ ) = 483.3 [ $\text{M} + \text{H}$ ] $^+$ , calcd. for  $\text{C}_{32}\text{H}_{27}\text{N}_4\text{O}$ : 483.2  $m/z$ .  $^1\text{H}$  NMR (dimethylformamide (DMF)- $d_7$ )  $\delta$ : 8.75 (2H, d,  $\text{H}_{23} + 33$ ), 8.72 (2H, d,  $\text{H}_4 + 12$ ), 8.58 (1H, s,  $\text{H}_{28}$ ), 8.60 (2H, d,  $\text{H}_1 + 15$ ), 8.12 (2H, d,  $\text{H}_{26} + 30$ ), 8.14 (2H, s,  $\text{H}_7 + 9$ ), 8.05 (2H, m,  $\text{H}_3 + 13$ ), 7.58 (2H, m,  $\text{H}_2 + 14$ ), 7.55 (4H, m,  $\text{H}_{24} + 32 + \text{H}_{25} + 31$ ), 4.90 (2H, s,  $\text{H}_{20}$ ), 5.55 (2H, t,  $\text{H}_{16}$ ), 3.41 (2H, t,  $\text{H}_{19}$ ) ppm;  $^{13}\text{C}\{^1\text{H}\}$  NMR (DMF- $d_7$ )  $\delta$ : 158.59 ( $\text{C}_6 + 10$ ), 157.29 ( $\text{C}_5 + 11$ ), 150.19 ( $\text{C}_1 + 15$ ), 138.85 ( $\text{C}_3 + 13$ ), 136.42 ( $\text{C}_{26}$ ), 130.42 ( $\text{C}_{30}$ ), 128.83 ( $\text{C}_{27} + 29$ ), 127.60 ( $\text{C}_{23} + 33$ ), 126.22 ( $\text{C}_{24} + 32$ ), 125.65 ( $\text{C}_{25} + 31$ ), 125.19 ( $\text{C}_4$ ), 123.13 ( $\text{C}_2 + 14$ ,  $\text{C}_{12}$ ), 108.67 ( $\text{C}_7 + 9$ ), 68.39 ( $\text{C}_{16}$ ), 50.00 ( $\text{C}_{20}$ ), 45.63 ( $\text{C}_{19}$ ) ppm.

### 2.1.2. Synthesis of 2-(2-([2.2':6',2''-terpyridin]-4'-yloxy)ethoxy)-N-(anthracen-9-ylmethyl)ethan-1-amine (AntPegTerp, $\mathbf{L}^2$ )

2-(2-(Anthracene-9-ylmethylamino)ethoxy)ethanol (2, AntPegOH) was synthesized as described above for compound **1**, using 2-(2-aminoethoxy)ethanol (1.2 mL, 12 mmol) instead of 2-aminoethanol. Yield: 2.674 g (91%).  $^1\text{H}$  NMR ( $\text{CDCl}_3$ - $d_3$ )  $\delta$ : 8.42 (1H, s,  $\text{H}_{28}$ ), 8.34 (2H, d,  $\text{H}_{23} + 33$ ), 8.01 (2H, d,  $\text{H}_{26} + 30$ ), 7.51 (4H, m,  $\text{H}_{24} + 32$ ,  $\text{H}_{25} + 31$ ), 4.79 (2H, s,  $\text{H}_{20}$ ), 3.66 (4H, dd,  $\text{H}_{17}$ ,  $\text{H}_{18}$ ), 3.54 (2H, m,  $\text{H}_{16}$ ), 3.04 (2H, t,  $\text{H}_{19}$ ), 2.28 (1H, s, NH) ppm.

AntPegTerp ( $\mathbf{L}^2$ ) was synthesized as described above for AntTerp ( $\mathbf{L}^1$ ) but starting from 2-(2-(anthracene-9-ylmethylamino)ethoxy)ethanol (0.295 g, 1 mmol). The final product was purified by column chromatography (100%  $\text{CH}_2\text{Cl}_2$  to 90/10  $\text{CH}_2\text{Cl}_2/\text{CH}_3\text{OH}$ ) being recovered as a pale brownish solid. Yield: 367 mg (78%). ESI-MS ( $\text{CH}_3\text{OH}$ ): ( $m/z$ ) = 527.4 [ $\text{M} + \text{H}$ ] $^+$ , calcd. for  $\text{C}_{34}\text{H}_{31}\text{N}_4\text{O}_2$ : 527.4  $m/z$ .  $^1\text{H}$  NMR (DMF- $d_7$ )  $\delta$ : 8.73 (2H, d,  $\text{H}_{23} + 33$ ), 8.69 (2H, d,  $\text{H}_4 + 12$ ), 8.54 (1H, s,  $\text{H}_{28}$ ), 8.50 (2H, d,  $\text{H}_1 + 15$ ), 8.09 (2H, d,  $\text{H}_{26} + 30$ ), 8.08 (2H, s,  $\text{H}_7 + 9$ ), 8.04 (2H, m,  $\text{H}_3 + 13$ ), 7.56 (2H, m,  $\text{H}_2 + 14$ ), 7.51 (4H, m,  $\text{H}_{24} + 32$ ,  $\text{H}_{25} + 31$ ), 4.78 (2H, s,  $\text{H}_{20}$ ), 4.48 (2H, t,  $\text{H}_{16}$ ), 3.96 (2H, d,  $\text{H}_{17}$ ), 3.79 (2H, t,  $\text{H}_{18}$ ), 3.09 (2H, t,  $\text{H}_{19}$ ) ppm;  $^{13}\text{C}\{^1\text{H}\}$  NMR (DMF- $d_7$ )  $\delta$ : 167.40 ( $\text{C}_8$ ), 157.45 ( $\text{C}_6 + 10$ ), 155.75 ( $\text{C}_5 + 11$ ), 149.58 ( $\text{C}_1 + 15$ ), 137.48 ( $\text{C}_3 + 13$ ), 132.81 ( $\text{C}_{21}$ ), 131.86 ( $\text{C}_{22} + 34$ ), 130.63 ( $\text{C}_{27} + 29$ ), 129.14 ( $\text{C}_{26} + 30$ ), 127.07 ( $\text{C}_{28}$ ), 126.11 ( $\text{C}_{23} + 33$ ), 125.28 ( $\text{C}_{24} + 32$ ), 125.05 ( $\text{C}_{25} + 31$ ), 124.69 ( $\text{C}_2 + 14$ ), 121.26 ( $\text{C}_4 + 12$ ), 107.28 ( $\text{C}_7 + 9$ ), 70.99 ( $\text{C}_{18}$ ), 69.29 ( $\text{C}_{17}$ ), 68.27 ( $\text{C}_{16}$ ), 49.63 ( $\text{C}_{20}$ ), 45.53 ( $\text{C}_{19}$ ) ppm.

### 2.1.3. Synthesis of anthracene-terpyridine-copper(II) complexes

To a solution of  $\mathbf{L}^1$  or  $\mathbf{L}^2$  (100 mg) in methanol (10 mL) was added  $\text{CuCl}_2 \cdot 5\text{H}_2\text{O}$  (1 equivalent). The mixture was stirred at room temperature for 3 h. The resulting green precipitates were recovered by filtration, washed with methanol and diethyl ether, and dried under vacuum.

2.1.3.1. AntTerpCu(II) ( $\text{CuL}^1$ ). Yield: 63 mg (49%). ESI-MS ( $\text{CH}_3\text{OH}$ ): ( $m/z$ ) = 652.4 [ $\text{M} + \text{Cl}$ ] $^-$ ; CHN (%): experimental 47.99 C, 4.37 H, 6.40 N; calculated for  $\text{C}_{32}\text{H}_{26}\text{Cl}_2\text{CuN}_4\text{O} \cdot 3\text{HCl} \cdot 5.5\text{H}_2\text{O}$  47.60 C, 4.74 H, 6.94 N.

2.1.3.2. AntPegTerpCu(II) ( $\text{CuL}^2$ ). Yield: 52 mg (41%). ESI-MS ( $\text{CH}_3\text{OH}$ ): ( $m/z$ ) = 696.3 [ $\text{M} + \text{Cl}$ ] $^-$ ; CHN (%): experimental 51.91 C, 5.18 H, 6.90 N; calculated for  $\text{C}_{34}\text{H}_{30}\text{Cl}_2\text{CuN}_4\text{O}_2 \cdot \text{HCl} \cdot 5\text{H}_2\text{O}$  51.85 C, 5.25 H, 7.11 N.

### 2.1.4. Synthesis of anthracene-terpyridine-platinum(II) complexes

2.1.4.1. Synthesis of cis-dichlorido(1,5-cyclooctadiene)platinum(II),  $[\text{Pt}(\text{cod})\text{Cl}_2]$ .  $\text{K}_2\text{PtCl}_4$  (1.000 g, 2.4 mmol) was dissolved in water (16 mL) and the resulting solution was filtered. To the filtered deep red solution, acetic acid (24 mL) and 1,5-cyclooctadiene (cod) (1.00 mL, 8.1 mmol) were added, in the dark. The reaction mixture was stirred and heated at ca. 90 °C in a water bath. Over 30 min the deep red solution slowly became pale yellow and some precipitation was observed. After ca. 2 h, the volume of the solution was reduced to 10 mL by evaporation under reduced pressure. The obtained precipitate was then centrifuged

and washed with water, ethanol and diethyl ether. Yield: 703 mg (80%).  $^1\text{H}$  NMR ( $\text{CDCl}_3$ - $d_3$ )  $\delta$ : 5.60 (4H, t, CH), 2.70 (2H, m,  $\text{CH}_2$ -CH), 2.30–2.16 (2H, m,  $\text{CH}_2$ -CH) ppm;  $^{13}\text{C}\{^1\text{H}\}$  NMR ( $\text{CDCl}_3$ - $d_3$ )  $\delta$ : 100.0 (CH), 30.0 ( $\text{CH}_2$ ) ppm;  $^{195}\text{Pt}$  NMR ( $\text{CDCl}_3$ - $d_3$ )  $\delta$ : -3340 ppm.

### 2.1.4.2. Synthesis of chlorido( $\mathbf{L}^1$ )platinum(II) chloride, $[\text{Pt}(\mathbf{L}^1)\text{Cl}]\text{Cl}$ ( $\text{PtL}^1$ )

To a suspension of  $[\text{Pt}(\text{cod})\text{Cl}_2]$  (93 mg, 0.25 mmol) in water (7 mL), a suspension of  $\mathbf{L}^1$  (115 mg, 0.24 mmol) in DMF (3 mL) was added with stirring, in the dark. After addition of the ligand, the color of the solution started to change from pale yellowish to orange. The reaction mixture was stirred and heated on a sand bath at 70 °C for 50 min. Thereafter, the reaction mixture was cooled to room temperature. The insoluble solids were removed by centrifugation and the red-orange clear supernatant solution was dried under vacuum. The resulting orange oil was stirred successively with diethyl ether to afford a microcrystalline orange solid. After removal of diethyl ether, the solid was dried under vacuum. Yield: 112 mg (62%). ESI-MS ( $\text{CH}_3\text{OH}$ )  $m/z$ : 713.7 [ $\text{M}$ ] $^+$ , calcd for  $\text{C}_{32}\text{H}_{26}\text{ClN}_4\text{OPt}^+$ : 713.14  $m/z$ .  $^1\text{H}$  NMR (DMF- $d_7$ )  $\delta$ : 9.053 (2H, d,  $\text{H}_4 + 12$ ), 8.773 (2H, d,  $\text{H}_1 + 15$ ), 8.563 (5H, m,  $\text{H}_{28}$  and  $\text{H}_2 + 14$  and  $\text{H}_{23} + 33$ ), 8.401 (2H, s,  $\text{H}_7 + 9$ ), 8.080 (4H, m,  $\text{H}_3 + 13$  and  $\text{H}_{26} + 30$ ), 7.559 (2H, d,  $\text{H}_{24} + 32$ ), 7.465 (2H, t,  $\text{H}_{25} + 31$ ), 4.940 (2H, s,  $\text{H}_{20}$ ), 4.761 (2H, t,  $\text{H}_{16}$ ), 3.5 (2H, t,  $\text{H}_{19}$ ) ppm;  $^{195}\text{Pt}$  NMR (DMF- $d_7$ )  $\delta$ : -2720 ppm.

### 2.1.4.3. Synthesis of chlorido( $\mathbf{L}^2$ )platinum(II) chloride, $[\text{Pt}(\mathbf{L}^2)\text{Cl}]\text{Cl}$ ( $\text{PtL}^2$ )

Compound  $\text{PtL}^2$  was synthesized using the same procedure as described above for  $\text{PtL}^1$ , by reacting  $[\text{Pt}(\text{cod})\text{Cl}_2]$  with  $\mathbf{L}^2$  (200 mg, 0.38 mmol). Yield: 182 mg (60%). ESI-MS ( $\text{CH}_3\text{OH}$ )  $m/z$ : 756.6 [ $\text{M}$ ] $^+$ , calcd for  $\text{C}_{34}\text{H}_{30}\text{ClN}_4\text{O}_2\text{Pt}^+$ : 756.17  $m/z$ .  $^1\text{H}$  NMR (DMF- $d_7$ )  $\delta$ : 8.753 (2H, d,  $\text{H}_4 + 12$ ), 8.625 (2H, d,  $\text{H}_1 + 15$ ), 8.460 (1H, s,  $\text{H}_{28}$ ), 8.432 (2H, t,  $\text{H}_2 + 14$ ), 8.368 (2H, d,  $\text{H}_{23} + 33$ ), 8.269 (2H, s,  $\text{H}_7 + 9$ ), 7.932 (2H, t,  $\text{H}_3 + 13$ ), 7.902 (2H, d,  $\text{H}_{26} + 30$ ), 7.445 (2H, t,  $\text{H}_{24} + 32$ ), 7.318 (2H, t,  $\text{H}_{25} + 31$ ), 4.826 (2H, s,  $\text{H}_{20}$ ), 4.761 (2H, t,  $\text{H}_{16}$ ), 4.141 (2H, t,  $\text{H}_{17}$ ), 3.976 (2H, t,  $\text{H}_{18}$ ), 3.286 (2H, t,  $\text{H}_{19}$ ) ppm;  $^{13}\text{C}\{^1\text{H}\}$  NMR (DMF- $d_7$ )  $\delta$ : 169.68 ( $\text{C}_8$ ), 158.51 ( $\text{C}_6 + 10$ ), 155.50 ( $\text{C}_5 + 11$ ), 151.37 ( $\text{C}_1 + 15$ ), 142.55 ( $\text{C}_3 + 13$ ), 131.50 ( $\text{C}_{22} + 34$ ), 130.59 ( $\text{C}_{27} + 29$ ), 129.32 ( $\text{C}_4 + 12$ ,  $\text{C}_{26} + 30$ ), 128.38 ( $\text{C}_{28}$ ), 126.50 ( $\text{C}_{23} + 33$ ), 126.06 ( $\text{C}_{24} + 32$ ), 1125.37 ( $\text{C}_{25} + 31$ ), 124.70 ( $\text{C}_2 + 14$ ), 111.26 ( $\text{C}_7 + 9$ ), 70.57 ( $\text{C}_{18}$ ), 69.39 ( $\text{C}_{17}$ ), 65.54 ( $\text{C}_{16}$ ), 49.11 ( $\text{C}_{20}$ ) ppm;  $^{195}\text{Pt}$  NMR (DMF- $d_7$ )  $\delta$ : -2700 ppm.

**Table 1**

Crystallographic data and refinement parameters for compound  $\mathbf{L}^1$ .

Empirical formula	$\text{C}_{32}\text{H}_{26}\text{N}_4\text{O}$
Formula weight	482.57
Temperature/K	150(2)
Crystal system	Triclinic
Space group	P1
a/Å	5.0226(2)
b/Å	10.5037(5)
c/Å	13.6134(6)
$\alpha$ /°	102.588(3)
$\beta$ /°	97.886(2)
$\gamma$ /°	102.783(2)
Volume/Å <sup>3</sup>	670.45(5)
Z	1
$\rho_{\text{calc}}/\text{cm}^3$	1.195
$\mu/\text{mm}^{-1}$	0.074
F(000)	254.0
Crystal size/mm <sup>3</sup>	0.2 × 0.16 × 0.12
$\theta$ range/°	2.89 to 25.68
Index ranges	-6 ≤ h ≤ 6, -12 ≤ k ≤ 11, -16 ≤ l ≤ 15
Reflections collected	6388
Independent reflections	3799 [ $R_{\text{int}} = 0.0199$ ]
Data/restraints/parameters	3532/4/338
Goodness-of-fit on $F^2$	1.059
Final R indexes [ $I > 2\sigma(I)$ ]	$R_1 = 0.0743$ , $wR_2 = 0.1369$
Final R indexes [all data]	$R_1 = 0.0756$ , $wR_2 = 0.1460$
Largest diff. peak/hole/e Å <sup>-3</sup>	0.202/-0.199
Flack parameter	0(2)

## 2.2. X-ray diffraction analysis

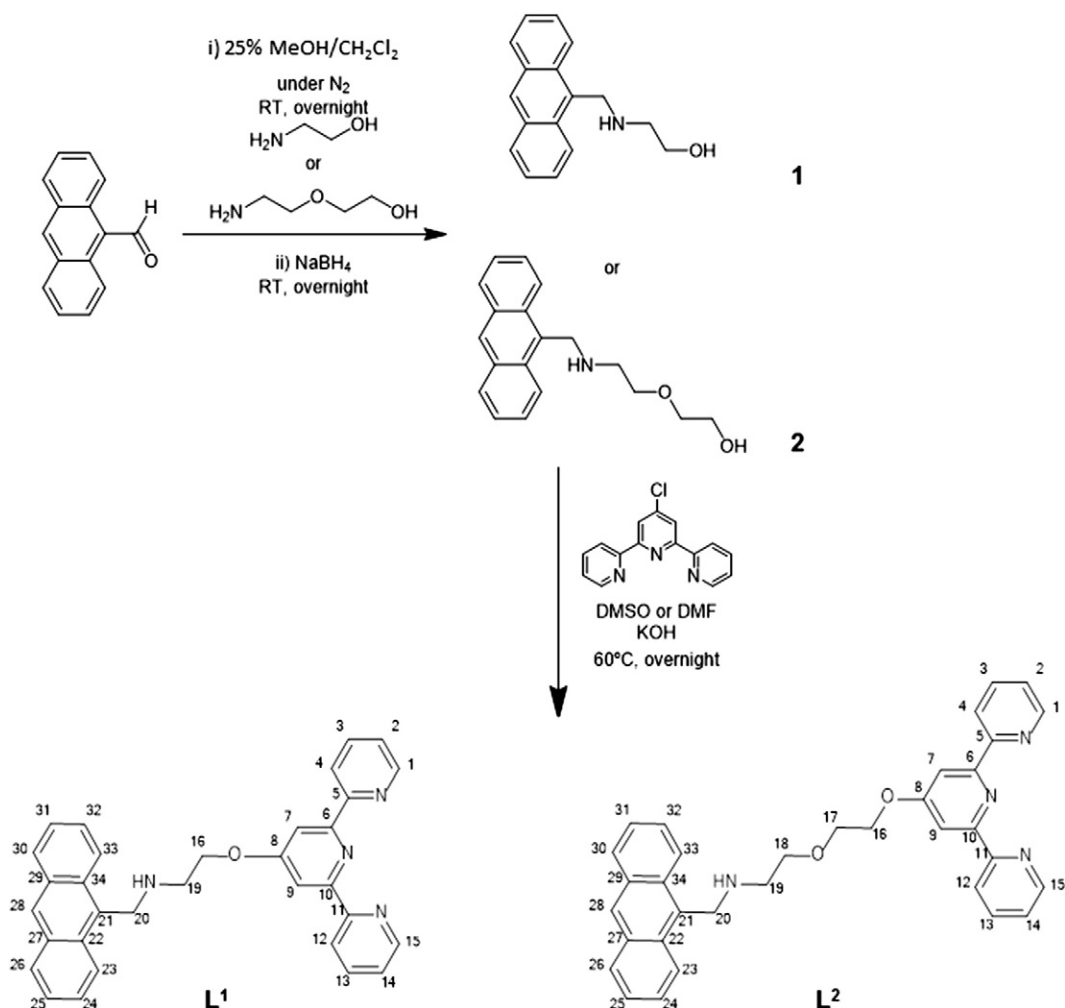
Crystals of **L**<sup>1</sup> suitable for X-ray diffraction studies were obtained from a concentrated dichloromethane solution of the compound, after standing for two days. The crystals were mounted on a loop with protective oil. X-ray data were collected at 150 K in the  $\omega$  and  $\varphi$  scans mode on a Bruker APEX II CCD diffractometer using graphite monochromated Mo K $\alpha$  radiation (0.71073 Å) and operating at 50 kV and 30 mA. Cell parameters were retrieved using Bruker SMART [41] software and refined using Bruker SAINT [41] on all observed reflections. Semi-empirical absorption corrections were applied using SADABS [42]. Structure solution and refinement were performed using direct methods with program SIR97 [43] and SHELXL97 [44], both included in the package of programs WINGX-Version 2013.3 [45]. A full-matrix least-squares refinement was used for the non-hydrogen atoms with anisotropic thermal parameters, except for disordered atoms that were refined isotropically. All hydrogen atoms were inserted in idealized positions and allowed to refine riding in the parent carbon atom. Molecular graphics were prepared using ORTEP3 [46]. A summary of the crystal data, structure solution and refinement parameters are given in Table 1. Crystallographic data for the structure of **L**<sup>1</sup> have been deposited at the Cambridge Crystallographic Data Centre as supplementary publication CCDC 1,431,619. Copies of the structures can be obtained free of charge from The Cambridge Crystallographic Data Centre via [www.ccdc.cam.ac.uk/data\\_request/cif](http://www.ccdc.cam.ac.uk/data_request/cif).

## 2.3. DNA interaction

### 2.3.1. Photophysical experiments

The labelled oligonucleotides HTelo DNA, (5'-FAM-AGGGTTAGGTTAGGGTTAGGG-TAMRA-3'), *c-myc* (5'-FAM-GGGGAGGGTGGGAGGGTGGG-TAMRA-3') and ds26 (5'-FAM-CAATCGGATCGAATTCGATCCGATTG-TAMRA-3') (FAM – fluorescein amidite, TAMRA – tetramethylrhodamine) were purchased from Eurogentec. The unlabelled oligos were also acquired from Eurogentec and Calf thymus DNA (ct-DNA) was purchased from Sigma Aldrich. Tested compounds were dissolved in DMSO to give 10 mM stock solutions. All solutions were stored in 100  $\mu$ L aliquots at –20 °C, thawed, and diluted immediately before use. Oligonucleotide concentrations were calculated using the following extinction coefficients ( $L\text{ cm}^{-1}\text{ mol}^{-1}$ ) at 260 nm given by the supplier: 220,590 (HTelo), 240,699 (*c-myc*), 258,900 (ds26), for quadruplex forming oligos per strand. The extinction coefficient of ct-DNA at 260 nm was taken to be 13,200  $L\text{ cm}^{-1}$  per base pair. [47].

**2.3.1.1. Fluorescence resonance energy transfer (FRET) assays.** FAM – TAMRA labelled DNA oligos were prepared as 20–30  $\mu$ M stock solutions in MilliQ water. Oligo DNA samples diluted to 0.40  $\mu$ M in lithium cacodylate (LiCad) buffer (pH 7.4). LiCad buffer was prepared from a stock solution of 10 mM LiOH, titrated with cacodylic acid until 7.4 pH was reached. To this solution, 1 mM KCl and 99 mM LiCl or 10 mM KCl and 90 mM LiCl were added to obtain the final buffer solution



**Scheme 2.** Synthesis of ligands **L**<sup>1</sup> and **L**<sup>2</sup>. The numbering schemes are those used to identify the <sup>1</sup>H and <sup>13</sup>C NMR signals.

**Table 2**  
Selected bond lengths (Å) and angles (°) for compound **L**<sup>1</sup>.

Length/Å						Angle/°							
Atom	Atom	Length	Atom	Atom	Length	Atom	Atom	Atom	Angle	Atom	Atom	Atom	Angle
O(1)	C(8)	1.367(5)	O(1)	C(16)	1.433(4)	C(8)	O(1)	C(16)	117.3(3)	O(1)	C(16)	C(17)	106.6(3)
N(1)	C(4)	1.339(5)	N(1)	C(5)	1.365(5)	C(4)	N(1)	C(5)	116.6(4)	N(1)	C(5)	C(6)	115.4(3)
N(2)	C(6)	1.339(4)	N(2)	C(10)	1.340(5)	C(6)	N(2)	C(10)	117.8(3)	C(1)	C(5)	C(6)	122.8(3)
N(3)	C(11)	1.364(5)	N(3)	C(15)	1.348(5)	N(2)	C(6)	C(5)	115.9(3)	N(3)	C(11)	C(10)	115.7(3)
N(4)	C(17)	1.466(5)	N(4)	C(18)	1.473(5)	N(2)	C(10)	C(11)	115.2(3)	C(12)	C(11)	C(10)	122.1(3)
C(5)	C(6)	1.489(5)	C(10)	C(11)	1.490(5)	C(11)	N(3)	C(15)	116.0(4)	C(20)	C(19)	C(18)	118.9(3)
C(16)	C(17)	1.514(6)	C(18)	C(19)	1.512(6)	C(17)	N(4)	C(18)	112.5(3)	C(32)	C(19)	C(18)	120.5(3)
						O(1)	C(8)	C(7)	124.1(3)	N(4)	C(17)	C(16)	111.0(3)
						O(1)	C(8)	C(9)	116.9(3)	N(4)	C(18)	C(19)	109.8(3)

used for *c-myc* oligo or HTelo and ds26, correspondingly. To anneal, samples were heated to 95 °C for 5 min, and allowed to cool slowly to room temperature overnight. *c-myc* was annealed in 1 mM KCl, 99 mM LiCl, 10 mM Lithium cacodylate and HTelo and ds26 in 10 mM KCl, 90 mM LiCl, 10 mM Lithium cacodylate buffer. For FRET melting experiments 8-well optical tube strips were used. The final volume of each sample was 40 µL, with a final DNA concentration of 0.20 µM and increasing concentration of tested compound (0–8 µM). In the case of the competition assays, each well was prepared with a final oligo concentration of 0.20 µM, 1 µM compound, and the ct-DNA concentration to test (0 to 120 µM). Measurements were performed on a PCR Stratagene Mx3005P (Agilent Technologies) with FAM excitation at 450–495 nm and detection at 515–545 nm. Readings were taken from 25 °C to 95 °C every 1 °C and at 1 °C/min melting rate. To obtain melting curves, normalised FAM fluorescence signal was plotted against temperature. From the non-linear fitting of the plot  $\Delta T_m [T_m (\text{with ligand}) - T_m (\text{without ligand})]$  obtained from at least three independent measurements] vs. ligand concentration, the  $\Delta T_m$  value for 1 µM concentration of ligand was obtained.

**2.3.1.2. Circular dichroism (CD).** CD titrations were done by adding a metal complex to test (0–50 µM) to the annealed *c-myc* or HTelo at 5 µM. To anneal, as previously described (Section 2.3.1.1) samples were heated to 95 °C for 5 min, and allowed to cool slowly to room temperature overnight. *c-myc* was annealed in 1 mM KCl, 99 mM LiCl, 10 mM Lithium cacodylate and HTelo in 10 mM KCl, 90 mM LiCl, 10 mM Lithium cacodylate buffer. CD experiments were performed on a Jasco J 810 spectropolarimeter using a 0.2 cm path length quartz cuvette and the spectra were recorded from 200 to 320 nm at 1 nm bandwidth.

**2.3.1.3. Spectroscopic titrations.** The electronic absorption spectra were obtained on a Perkin-Elmer UV/Vis spectrometer and fluorescence spectra on a Varian Cary-Eclipse, all in quartz cuvettes (1 cm). Spectroscopic studies were performed in 50 mM Tris HCl buffer (pH 7.4) with 10 mM KCl at  $20 \pm 0.5$  °C. Titrations were performed keeping a constant concentration of the compound (2.5 and 15 µM for emission and absorption, respectively) and concentrated DNA was then added to the solution containing the compound until changes in the absorbance/emission became noticeably indifferent. Samples were excited at 368 nm, where upon titration of DNA, absorbance changes were negligible. Emission spectra were recorded from 380 to 600 nm. Two independent repeats were performed. Binding data obtained from spectrophotometric and spectrofluorimetric titrations were cast into Scatchard plot of  $r/C_f$  versus  $r$ . Non-linear binding isotherms observed were fitted to a theoretical curve drawn according to the excluded site model developed by McGhee and von Hippel [48].

### 2.3.2. Polymerase stop assay (PSA)

The oligonucleotide containing a quadruplex-forming sequence derived from *c-myc* oncogene (5'-GCGGCTCCTGTGAGGGTGGGGAGG

GTGGGGAAGATTCCCGACTTCGTATTAAGTACTCTAGCCTT-3') and the corresponding partially complementary FAM label-sequence (5'-FAM-AAGGCTAGAGTACTTAATACGA-3') were used. A mixture of each oligonucleotide (1 µM each) and increasing concentrations of the compounds (0, 0.3, 1, 2.5, 5, 10 and 20 µM) were annealed in TRIS (Tris(hydroxymethyl)aminomethane)-HCl buffer (50 mM, pH 7.4). After cooling to room temperature, the PSA reactions were performed in 1× Taq (*Thermus aquaticus*) buffer, containing the previously annealed solution (0.2 µM), dNTPs (deoxyribose nucleotide triphosphates (0.2 mM), MgCl<sub>2</sub> (1.25 mM) and Taq DNA polymerase (2.5 U) at 37 °C during 30 min. The reactions were quenched by adding an equal volume of stop buffer (90% formamide, 10 mM NaOH). PSA products were then analysed on a denaturing polyacrylamide gel (20%) in 1× TBE (Tris/Borate/EDTA) and visualized with FAM dye. As a control experiment, a non-forming quadruplex sequence was used (5'-GCGGCTCCTGTGAGGGTGAAGAGGGTGGGGA AGATTCCCGACTTCGT ATTAAGTACTCTAGCCTT-3').

## 3. Results and discussion

### 3.1. Synthesis of anthracene-terpyridine chelators and the corresponding M(II) (M = Cu, Pt) complexes

The anthracene-terpyridine chelators (**L**<sup>1</sup> and **L**<sup>2</sup>) were obtained using 4'-chloro-2,2':6',2''-terpyridine as starting material, which was O-alkylated using the appropriate alcohol derivative of 2-aminomethylanthracene via a Williamson reaction (Scheme 2). The alcohol derivatives of anthracene, compounds **1** and **2** containing an ethylenic or pegylated linker, respectively, were synthesized by reduction

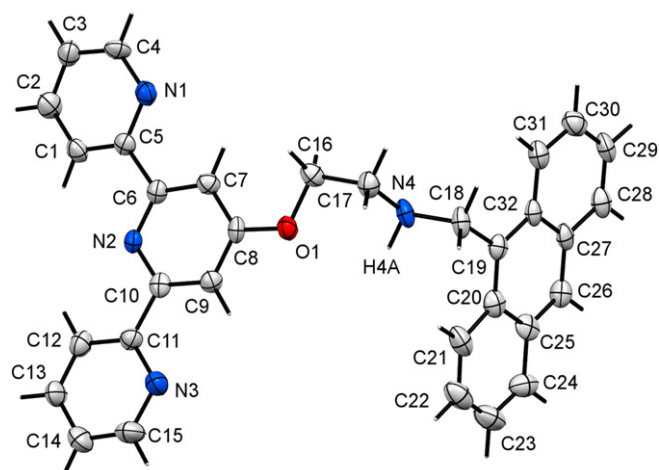


**Fig. 1.** ORTEP diagram of **L**<sup>1</sup>. Ellipsoids were drawn at the 50% probability level.

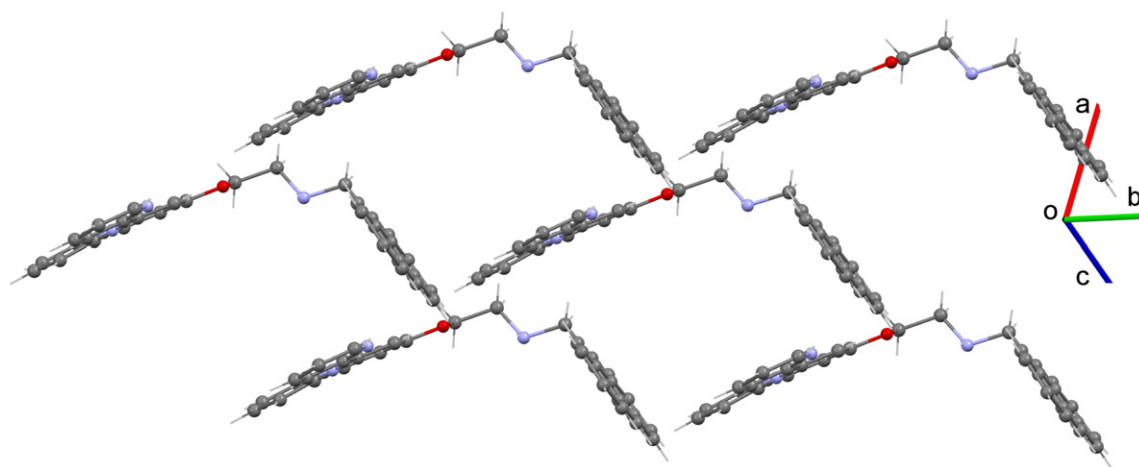


Fig. 2. Pack diagram of  $L^1$ .

of the imine function of the corresponding Schiff base precursors, as shown in Scheme 2.

The chemical identity of compounds  $L^1$  and  $L^2$  was ascertained based on their characterization by  $^1H$  and  $^{13}C$  NMR spectroscopy and by ESI-MS. For  $L^1$ , X-ray diffraction analysis confirmed the proposed formulation. X-ray quality crystals of  $L^1$  were obtained by recrystallization from a saturated solution of the compound in dichloromethane.  $L^1$  crystallized in a triclinic system, space group  $P1$  with one independent molecule in the asymmetric unit. The crystal data and final refinement details are given in Table 1. A selection of bond lengths and angles are given in Table 2. The respective ORTEP diagram is presented in Fig. 1.

The molecular structure of  $L^1$  is defined by two almost planar fragments, terpyridine and anthracene, connected by a spacer (Fig. 1). These two planar units are almost perpendicular to each other, with a dihedral angle between the respective l.s. planes of  $77.70(4)^\circ$  as illustrated in Fig. 2. The three pyridine rings present a *trans-trans* configuration and are not coplanar. The dihedral angles between the l.s. planes of the rings containing atoms N1 and N2, and atoms N2 and N3 are  $4.25(2)^\circ$  and  $8.91(2)^\circ$ , respectively. Several short  $C-H\cdots O$  or  $C-H\cdots C$  contacts between adjacent molecules give rise to a three-dimensional network as shown in Fig. 3.

The synthesized new anthracene-terpyridine (Ant-tpy) chelators,  $L^1$  and  $L^2$ , were used to obtain complexes of the type  $[Cu(\text{Ant-tpy})Cl_2]$  and  $[Pt(\text{Ant-tpy})Cl]^+$ . As mentioned in the introductory section, we have considered that the presence of metal centres with different geometry would influence the affinity and selectivity of metallated anthracene-terpyridine derivatives towards DNA structures of different topology. For example, Teulade-Fichou et al. have shown previously that the complex  $[Cu(\text{ttpy})(NO_3)_2]$  (ttpy = tolyl-terpyridine) has a higher selectivity for G-quadruplex DNA over duplex DNA if compared with the Pt(II) counterpart  $[Pt(\text{ttpy})Cl]^+$ . This difference was accounted by the square pyramidal coordination geometry of the Cu(II) complex that might hinder intercalation between two pairs of duplex DNA, unlike the square planar Pt(II) congener that has the propensity to act as a DNA intercalator [34]. Similar results were obtained by Vilar et al. with a different set of copper(II) and platinum(II) terpyridine complexes [36,39,40].

The copper complexes ( $CuL^1$  and  $CuL^2$ ) were obtained by reacting stoichiometric amounts of the desired anthracene-terpyridine chelator and copper(II) chloride in methanol at room temperature (Scheme 3), using a similar approach to the one described originally to synthesize the simplest member of this family of coordination complexes,  $[Cu(\text{tpy})Cl_2]$  [49]. The formation of  $CuL^1$  and  $CuL^2$  was almost

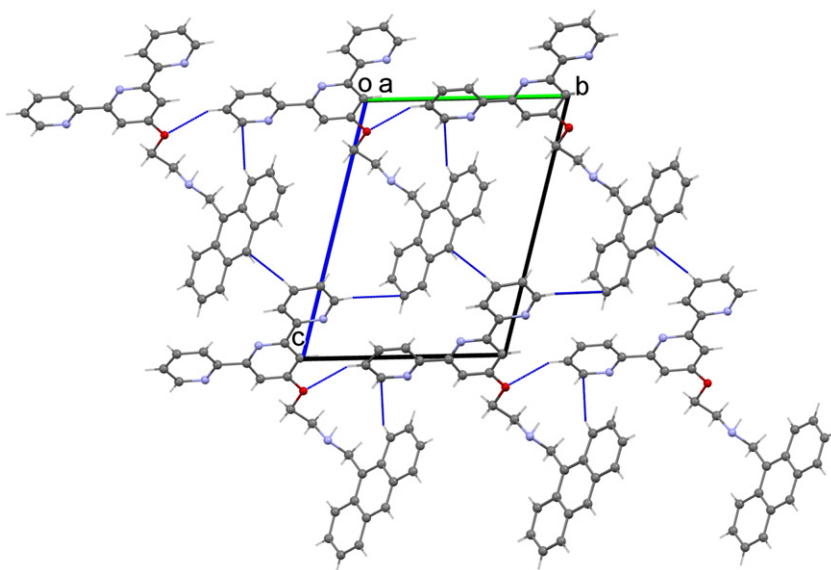
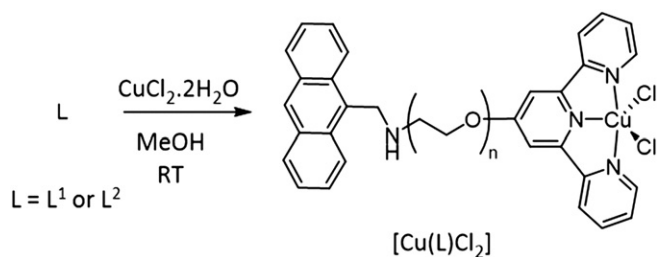


Fig. 3. Pack diagram of  $L^1$  showing short  $C-H\cdots C$  and  $C-H\cdots O$  contacts ( $C3-H3\cdots O1 = 2.635$ ,  $C13-H13\cdots C26 = 2.683$ ,  $C15-H15\cdots C29 = 2.791$ ,  $C21-H21\cdots C4 = 2.761$ ).



**Scheme 3.** Synthesis of Cu(II) complexes.

immediate as indicated by the sudden appearance of a green color upon addition of ligands. The complexes precipitated from each reaction mixture as a green solid, and were characterized by ESI-MS and elemental analysis. The negative ion mode ESI-MS spectra of **CuL<sup>1</sup>** and **CuL<sup>2</sup>** have shown major peaks corresponding to the  $[M + Cl]^-$  ions with the expected isotopic distribution pattern. This finding corroborated the formation of the desired Cu(II) complexes having a single anthracene-terpyridine coordinated ligand.

The Pt(II) compounds with the Ant-tpy chelators were synthesized according to a procedure based on a method described by Annibale et al. [50] for the synthesis of the congener  $[Pt(tpy)Cl]Cl$ . In this method,  $[Pt(cod)Cl_2]$  [51] was used as the starting precursor; the precursor rapidly reacted with **L<sup>1</sup>** and **L<sup>2</sup>** to afford **PtL<sup>1</sup>** and **PtL<sup>2</sup>**, which were recovered in moderate yield (ca. 60%) as orange solids (Scheme 4). We have found that the use of a small excess of platinum (ca. 3%) and a longer reaction time (50 min vs. 15 min) increased the yield of our synthesis (from 25% to ca. 60%) if compared with the synthesis carried out using the conditions originally reported to obtain the parental complex  $[Pt(tpy)Cl]Cl$ .

The chemical identity of the newly synthesized Pt(II) complexes was ascertained by LC-MS and by multinuclear NMR spectroscopy. For both complexes the positive ESI-MS spectra in methanol have shown the presence of intense peaks corresponding to the cationic species  $[Pt(L)Cl]^+$  ( $L = L^1$  and  $L^2$ ). By comparing the <sup>1</sup>H and <sup>13</sup>C NMR spectra of **PtL<sup>1</sup>** and **PtL<sup>2</sup>**, obtained using freshly prepared solutions of the complexes, with the spectra of the corresponding ligand in the same solvent, we observed a downfield shift in the peaks correspondent to the terpyridine protons and carbons, namely for the 1/15 (<sup>1</sup>H:  $\Delta\delta = 0.25$  ppm, <sup>13</sup>C:  $\Delta\delta = 1.80$  ppm), 2/14 (<sup>1</sup>H:  $\Delta\delta = 0.37$ ), and 3/13 (<sup>1</sup>H:  $\Delta\delta = 0.39$  ppm; <sup>13</sup>C:  $\Delta\delta = 5.06$ ) carbon/hydrogen atoms (see Scheme 2 for atom numbering), due to the influence of the metal-ligand bond. The <sup>195</sup>Pt{<sup>1</sup>H} NMR spectrum exhibited only one signal for each compound ( $-2720$  ppm for **PtL<sup>1</sup>** and  $-2700$  ppm for **PtL<sup>2</sup>**)

with chemical shifts that are well in agreement with the values reported in the literature for  $[Pt(tpy)Cl]$  ( $-2694$  ppm [52]).

### 3.2. Biophysical studies: evaluation of G-quadruplex DNA binding

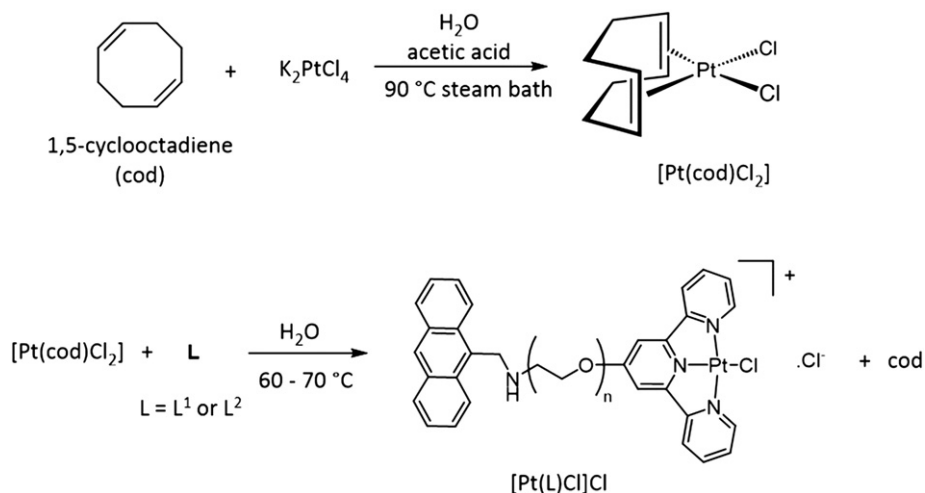
We have investigated the DNA binding of **PtL<sup>1,2</sup>** and **CuL<sup>1,2</sup>** in comparison with the respective metal-free ligands, **L<sup>1</sup>** and **L<sup>2</sup>**, using a variety of techniques (FRET melting studies, UV/Vis, CD and fluorescence titrations, and polymerase stop assay). We also compared these results with previously reported DNA binding studies with other metal-terpyridine complexes.

#### 3.2.1. Fluorescence resonance energy transfer (FRET)

Fluorescence resonance energy transfer (FRET) melting studies were conducted to investigate the effect of the four metal complexes (**PtL<sup>1,2</sup>** and **CuL<sup>1,2</sup>**) on the stability of two G-quadruplex DNA structures, namely human telomeric (HTelo) and *c-myc* promoter (*c-myc*) sequences (see Experimental Details for exact sequences). In addition, the affinity of these compounds towards a duplex DNA sequence (ds26) was also assessed. FRET melting curves of HTelo, *c-myc* and ds26 were obtained (Figs. S1–S3) and melting temperature differences ( $\Delta T_m$ ) (see Table 3) were determined, with increasing concentrations (from 0 to 10  $\mu$ M) of the tested compounds. As shown in Table 3, the metal complexes induce some stabilization of G-quadruplex (HTelo and *c-myc*); in contrast, they presented very low values of  $\Delta T_m$  with the duplex DNA sequence.

To evaluate the effect of the metal on quadruplex DNA stabilization, the corresponding metal-free ligands were also analysed under the same experimental conditions (Table 3). The  $\Delta T_m$  values at 1  $\mu$ M obtained for **L<sup>1</sup>** and **L<sup>2</sup>** are lower than the  $\Delta T_m$  values obtained for the corresponding metal complexes; particularly, in case of the Pt(II) complexes and with the *c-myc* sequence where the  $\Delta T_m$  values are ca. 3-fold (**L<sup>1</sup>** vs **PtL<sup>1</sup>**) or 7-fold (**L<sup>2</sup>** vs **PtL<sup>2</sup>**) higher for the complexes. These results show that the presence of the metal is essential for high affinity (and selectivity) to quadruplex. This effect is more evident in the case of the platinum(II) complexes, which display selectivity for *c-myc* quadruplex DNA not only over duplex DNA but also over HTelo quadruplex DNA. Moreover, the presence of a longer linker between the chelating terpyridine unit and the anthracene moiety enhances the interaction with G-quadruplex-forming sequences.

The selectivity G-quadruplex vs. duplex DNA was also evaluated and confirmed by competition FRET melting assays where increasing amounts of ct-DNA were added to a fixed mixture of FRET-labelled G-quadruplex oligo and metal complex (at 1  $\mu$ M concentration). No significant change to the  $\Delta T_m$  values were observed upon addition of 300 equivalents of ct-DNA and in some cases (mainly with *c-myc*



**Scheme 4.** Synthesis of Pt(II) complexes.

DNA) even after addition of 600 equivalents of ct-DNA. This confirms the selectivity of the tested Pt(II) and Cu(II) compounds to the G-quadruplexes (Fig. 4).

The results obtained suggest that the inclusion of the anthracenyl moiety in the terpyridine-metal complex system seems to increase the interaction with G-quadruplexes when compared with simple platinum(II) or copper(II) terpyridine complexes, i.e. without any substituents in the aromatic ring. Some of our complexes display  $\Delta T_m$  values that are similar to those exhibited by toluene-terpyridine Pt(II) and Cu(II) derivatives (see Table S1 in the SI). For the later complexes, their augmented G-quadruplex interaction was associated with the extension of the interlinked aromatic system with consequent increase of  $\pi$ - $\pi$  interactions. This is not likely to occur with the Pt(II) and Cu(II) complexes described herein as the anthracenyl ring is attached to the tpy unit using flexible linkers of different length. One possibility is that the anthracenyl moiety interacts via  $\pi$ - $\pi$  stacking with bases present in the loops of the G-quadruplex structure providing higher affinity and distinct selectivity to the metal-terpyridine complexes. However, further studies will be required to clarify the exact binding mode of the new complexes.

### 3.2.2. CD measurements

To study the effect of metal complexes on the HTelo and *c-myc* quadruplex structures, CD titrations were carried out. It is known that G-quadruplexes can exist in solution as a mixture of different topologies (e.g. parallel and antiparallel G4s). The spectra of parallel quadruplexes have a dominant positive band at 260 nm, whereas the spectra of antiparallel quadruplexes have a negative band at 260 nm and positive band at 290 nm. In presence of  $K^+$ , HTelo DNA adopts an antiparallel/parallel hybrid conformation and exhibits a maximum at 290 nm and a “shoulder” at around 260 nm. With the addition of the metal complexes (1–10 eq) to HTelo quadruplex, the negative band at 260 nm appeared and a decrease of the 290 nm band was observed, suggesting a change in the conformation of HTelo quadruplex induced by the binding of the metal complexes. *C-myc* quadruplex in the presence of  $K^+$  adopts a predominantly parallel conformation. Addition of metal complexes resulted in the decrease of the positive band intensity at 260 nm, suggesting interaction with the structure (see Fig. 5 for a representative example). Overall CD titration experiments suggest that the metal complexes interact with HTelo and *c-myc* quadruplex. It should be noted that at higher concentrations, compound precipitation was observed.

### 3.2.3. Spectrofluorimetric titrations

In order to quantify the affinity of the compounds towards quadruplex and duplex structures, we performed fluorimetric titrations with duplex DNA (ct-DNA) and G-quadruplex DNA sequence *c-myc*. Upon addition of *c-myc* DNA to solutions of the corresponding metal complex, a decrease in the emission intensity was observed. In contrast, an increase in fluorescence emission was observed upon addition of G4 to **L**<sup>1</sup> or **L**<sup>2</sup> solutions (Fig. 6 and S6 in SI). The different emission behaviours between the free ligands and the metal complexes could be related to differences in energy

**Table 3**

$\Delta T_m$  for 1  $\mu$ M concentration of compound. Values determined from fitting average  $\Delta T_m$  points<sup>a</sup> obtained from FRET melting curves of labelled DNA oligomers in the presence of the different compounds.

	$\Delta T_m$ /°C		
	ds26	HTelo	<i>c-myc</i>
<b>L</b> <sup>1</sup>	0.68 ± 0.76	2.91 ± 0.54	2.98 ± 0.68
<b>PtL</b> <sup>1</sup>	0.00 ± 0.65	9.42 ± 0.56	10.22 ± 0.56
<b>CuL</b> <sup>1</sup>	0.00 ± 0.84	5.31 ± 0.45	2.07 ± 0.65
<b>L</b> <sup>2</sup>	0.53 ± 0.38	5.00 ± 0.70	2.5 ± 1.0
<b>PtL</b> <sup>2</sup>	0.39 ± 0.81	9.57 ± 0.49	15.60 ± 0.70
<b>CuL</b> <sup>2</sup>	0.58 ± 0.79	5.92 ± 0.65	7.26 ± 0.27

<sup>a</sup> ± std. dev. on a minimum of three replicates.

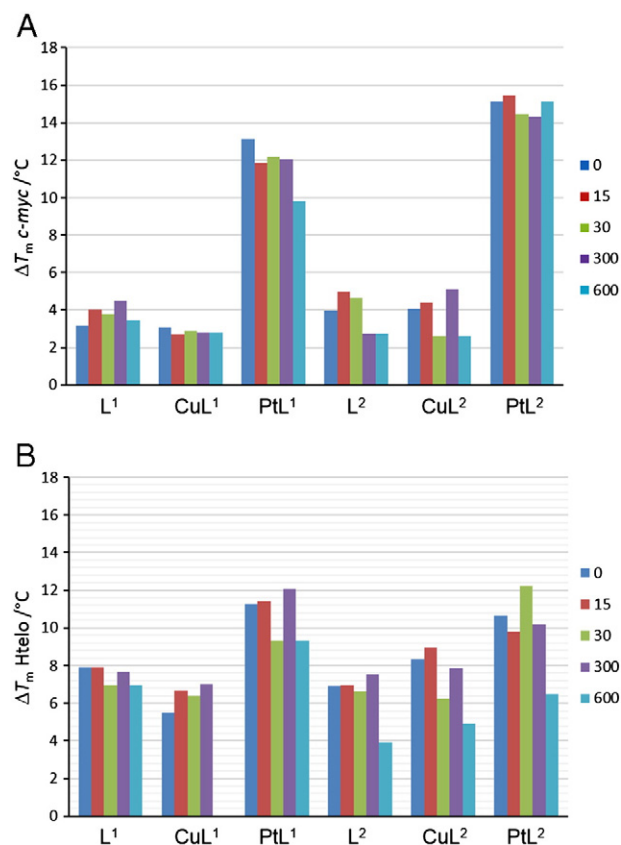


**Fig. 4.** FRET competition experiments of selected complexes at 1  $\mu$ M concentration showing the variation ( $\Delta T_m$ ) of a) FAM-*c-myc*-TAMRA and b) FAM-HTelo-TAMRA DNA melting temperature with increased concentration (0–120  $\mu$ M) of ct-DNA (corresponding to 0 to 600 equivalents).

transfer processes between the fluorophore and the terpyridine/metal-terpyridine. A similar behaviour has been reported by Bonnet et al. for a metal-terpyridine system attached to a fluorophore where some energy absorbed by the fluorophore is donated to the metal centre whilst in the metal-free terpyridine system, this process is hampered [53]. Further studies will have to be carried out to characterise fully the photophysical behaviour of these compounds upon DNA binding.

An analogous behaviour was observed upon addition of ct-DNA: a decrease in the emission of the metal complexes (**CuL**<sup>1</sup>, **PtL**<sup>1</sup>, **CuL**<sup>2</sup> and **PtL**<sup>2</sup>) was observed upon increasing amounts of ct-DNA (Fig. S7 in SI) while a very large increase in emission was observed for the metal-free ligands (**L**<sup>1</sup> and **L**<sup>2</sup>). Absorption titrations for these compounds were conducted to obtain the affinity constants (Fig. S8).

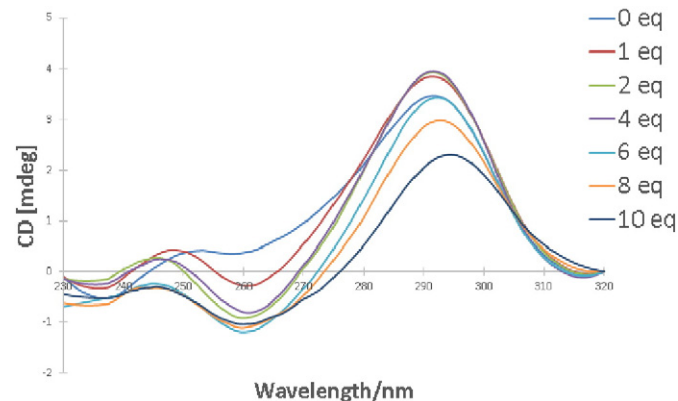


**Fig. 5.** CD spectra of 5  $\mu$ M HTelo DNA recorded in the presence of different concentrations of **PtL**<sup>2</sup> in LiCac pH 7.2 buffer (KCl 10 mM, LiCl 90 mM, lithium cacodylate 10 mM).

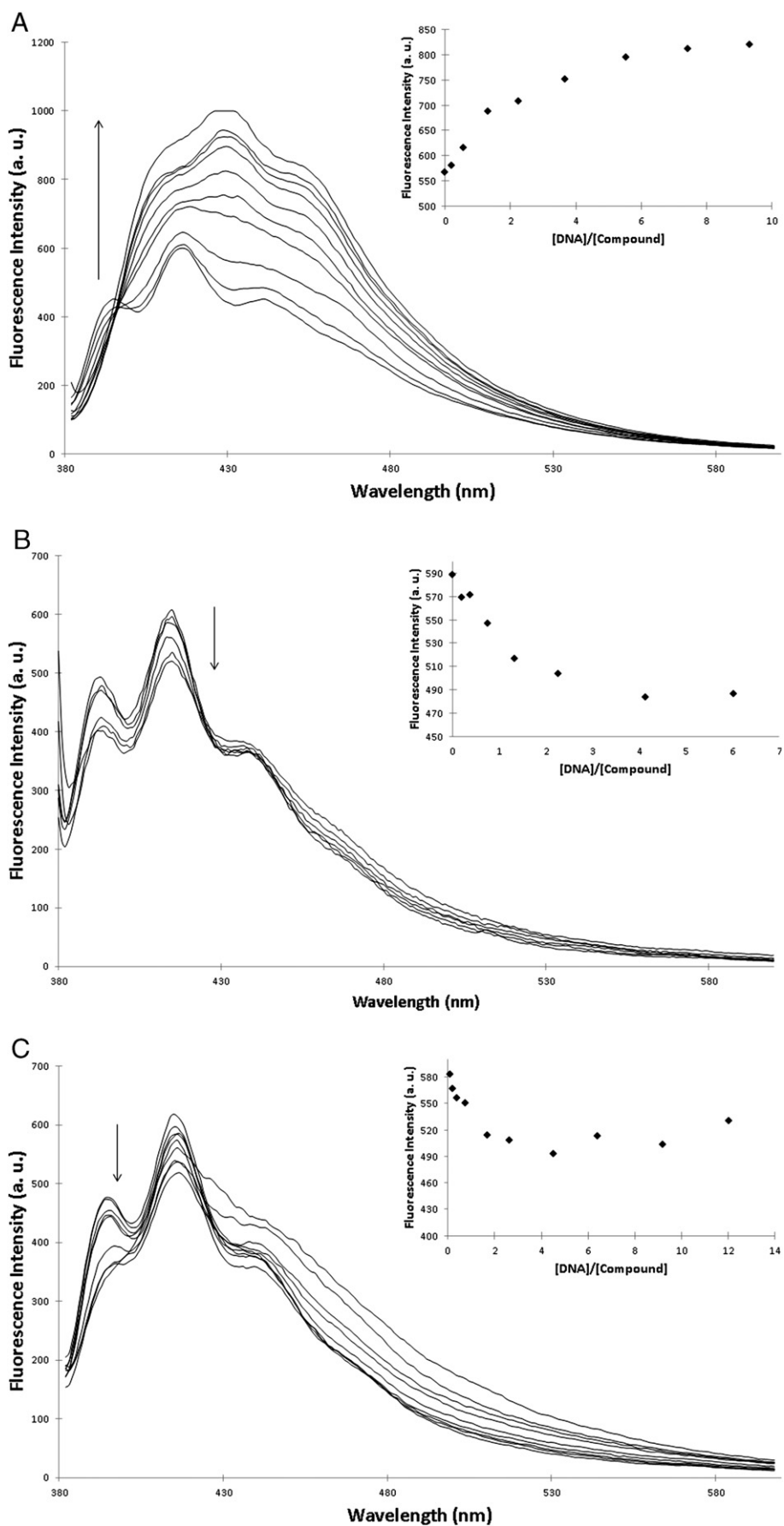


**Fig. 6.** Spectrofluorimetric titrations of *c-myc* quadruplex DNA with (a)  $L^2$ , (b)  $CuL^2$  and (c)  $PtL^2$  in Tris HCl buffer (Tris HCl 50 mM, pH 7.4, KCl 10 mM). Insets show the plotting of emission fluorescence at 412 nm vs. molar ratio ([DNA]/[Compound]).

**Table 4**  
Binding constants<sup>a</sup> (log Ks) calculated from the spectroscopic titrations of compounds with *c-myc* quadruplex DNA and calf thymus DNA.

Compound	<i>c-myc</i>	Calf thymus DNA
<b>L<sup>1</sup></b>	3.11 <sup>b</sup>	5.17
<b>CuL<sup>1</sup></b>	5.62	4.89
<b>PtL<sup>1</sup></b>	5.82	5.22
<b>L<sup>2</sup></b>	3.71 <sup>b</sup>	4.99
<b>CuL<sup>2</sup></b>	6.13	5.17
<b>PtL<sup>2</sup></b>	6.32	5.16

<sup>a</sup> Processing of titration data by means of Scatchard equation.

<sup>b</sup> Data obtained from UV–Vis titrations.

The affinity binding constants were calculated through Scatchard plot analysis and are shown in Table 4. The log K values ranged from 3.1 to 6.1 depending on the compound and DNA structure used. The log K values confirm the  $\Delta T_m$  obtained by FRET: the metal complexes have significantly higher affinities (log K  $\approx$  5.6–6.3) than the metal-free ligands (log K  $\approx$  3.1–3.7), highlighting the important role the metal centre plays. We hypothesise that the metal centre ‘forces’ the terpyridine moiety into a planar arrangement thus making available for efficient  $\pi$ -stacking. Compounds with a longer linker (**L<sup>2</sup>**, **CuL<sup>2</sup>** and **PtL<sup>2</sup>**) display higher affinities than those with the shorter linker (**L<sup>1</sup>**, **CuL<sup>1</sup>** and **PtL<sup>1</sup>**). Furthermore, the Pt(II) complexes also display higher log K values towards *c-myc* quadruplex DNA than the Cu(II) complexes [54,55].

### 3.2.4. Polymerase stop assay

In order to evaluate the ability of the compounds to form a G-quadruplex structure as part of a longer sequence, we performed polymerase stop assays. As has been discussed elsewhere [56], in this assay a polymerase enzyme is added to a mixture of a labelled primer and a DNA template which contains a quadruplex forming sequence. The polymerase is able to extend the full length of the template if no quadruplex forms. However, if a stable quadruplex is formed (e.g. by adding mM concentrations of K<sup>+</sup>-lane 8 in Fig. 7 – or a quadruplex-stabilising ligand – lanes 3–7 in Fig. 7) in the template sequence, the polymerase stops at the point where the quadruplex forms. Therefore, the length of the oligonucleotides formed in this assay is an indication of whether a stable quadruplex forms or not. Fig. 7 shows the PAGE

(polyacrylamide gel electrophoresis) gels obtained after running the polymerase stop assay in the presence of **CuL<sup>2</sup>** (see SI for **L<sup>1</sup>**, **L<sup>2</sup>** and **CuL<sup>1</sup>**). The relative intensities of the band associated to the shorter oligonucleotide formed (i.e. the one formed up to the point that the quadruplex forms) were plotted and the values corresponding to the 50% of ‘G4 band’ formation in relation to the control (i.e. the system in the absence of ligand or K<sup>+</sup>) were calculated. It should be noted that even at the highest concentration of **CuL<sup>2</sup>**, we did not see a significant decrease (ca. 30%) of the upper band associated to the oligo formed if G-quadruplex is not formed. This suggests that **CuL<sup>2</sup>** is not a particularly strong G-quadruplex binder, which is consistent with the other biophysical data (see above). It should be noted that when we carried out polymerases stop assays with the platinum complexes **PtL<sup>1</sup>** and **PtL<sup>2</sup>**, precipitation was observed and hence these two complexes could not be studied using this assay (Figs. S9–10 in SI).

The polymerase stop assays show that the copper complexes have the ability to halt polymerase – upon stabilization of the G-quadruplex – at lower concentrations (EC<sub>50</sub> 3.18  $\mu$ M and 1.34  $\mu$ M for **CuL<sup>1</sup>** and **CuL<sup>2</sup>** respectively) than the metal-free ligands (EC<sub>50</sub> for both **L<sup>1</sup>** and **L<sup>2</sup>** > 20  $\mu$ M). These results also show that **CuL<sup>2</sup>** is more efficient at stopping the activity of polymerase than **CuL<sup>1</sup>**. These results are consistent with the biophysical studies presented in the previous sections.

To confirm that the halting of the polymerase activity was due to quadruplex formation, a control experiment was carried out where the polymerase stop assay was performed with a template oligonucleotide which does not containing a quadruplex-forming sequence (Fig. S10). This experiment didn’t show any polymerase pausing product in the presence of **L<sup>1</sup>**, **L<sup>2</sup>**, **CuL<sup>1</sup>** or **CuL<sup>2</sup>** indicating that the EC<sub>50</sub> values obtained in the presence of the copper(II) complexes (see above) are due to the formation of quadruplexes.

## 4. Conclusions

The new Pt(II) and Cu(II) complexes herein reported showed affinity for quadruplex-forming sequences (HTelo and *c-myc*) with a good selectivity over duplex DNA (ds26 and ct-DNA), as shown by the FRET assays. Importantly, the metal-free ligands do not have significant affinity to any of the DNA sequences investigated, which shows that the

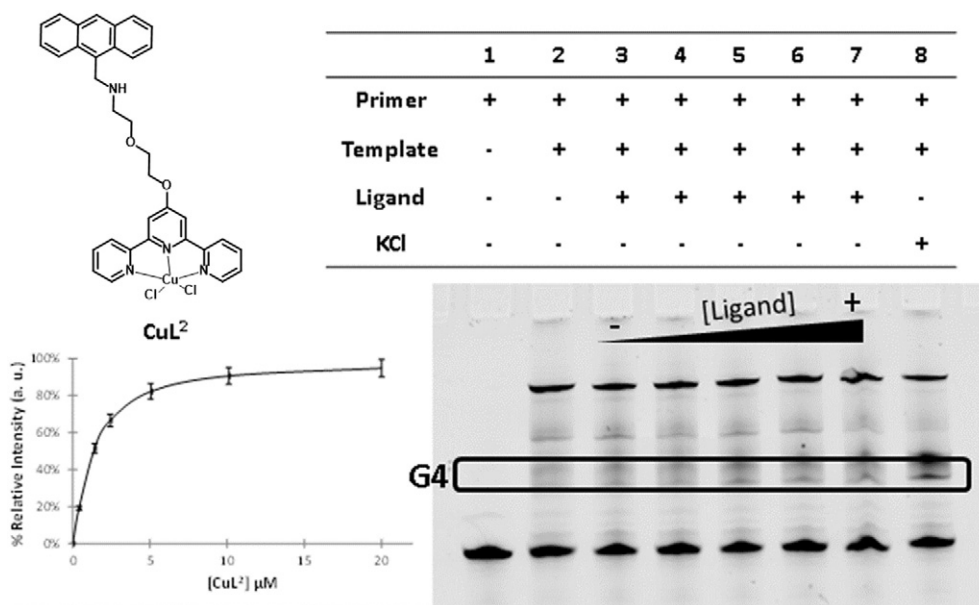


**Fig. 7.** Polymerase Stop Assay of the *c-myc* sequence in the presence of **CuL<sup>2</sup>** highlighting the bands (enclosed in rectangle) corresponding to the shorter oligonucleotide obtained when quadruplexes form. The 1st lane shows the primer, the 2nd lane shows the mixture of primer and template, lanes 3 to 7 show the result of the polymerase assay upon mixing the primer, template and increasing concentrations of compound; the 8th lane shows the result of the assay with the primer, template and K<sup>+</sup>. The plot of the relative intensities vs. concentration of compound is on the left.

presence of the metal is essential for high affinity (and selectivity). This effect is more evident in the case of the platinum(II) complexes. Moreover, the presence of a longer linker between the chelating terpyridine unit and the anthracene moiety enhances the interaction with G-quadruplex-forming sequences. These trends were further corroborated and quantified by the determination of the affinity binding constants for the interaction of the different compounds with G-quadruplex and duplex DNA structures, which were measured based on fluorescence and spectrophotometric titrations.

Interestingly, the [Pt(Ant-tpy)Cl]<sup>+</sup> complexes described herein targets the G-quadruplex DNA structures more selectively than the copper analogue, [Cu(Ant-tpy)Cl<sub>2</sub>], despite the expected better ability of the planar [Pt(tpy)Cl]<sup>+</sup> unit to intercalate between adjacent base pairs of duplex DNA if compared with the [Cu(Ant-tpy)Cl<sub>2</sub>] unit. Altogether, these results point out that the affinity and selectivity of these anthracene-containing M(II)-tpy (M = Cu, Pt) complexes towards G-quadruplex DNA structures are certainly justified by an intricate interplay of effects such as  $\pi$ -stacking with the accessible G-tetrad or with loops and grooves of the quadruplex DNA elements, as well as electrostatic interactions involving the more polar pendant arm.

Our results indicate that the combination of the terpyridine scaffold linked to a 'classical' DNA intercalator can afford metal(II) complexes with affinity and selectivity for G-quadruplex DNA. This effect needs to be better explored, in particular in order to clarify whether the anthracenyl and metal-terpyridine moieties are acting in a synergistic way when the complexes bind to G-quadruplexes. Nevertheless, these encouraging results give impetus to pursue with these studies using different pendant intercalators, namely those having a more extended aromatic structure and/or a cationic nature that might improve the binding affinity and water solubility of the final compounds. It should be noted that when.

#### Abbreviations list

Ant	Anthracene
AntOH and/or <b>1</b>	2-(anthracen-9-ylmethylamino)ethanol
AntTerp and/or <b>L<sup>1</sup></b>	2-([2,2':6',2''-terpyridin]-4'-yloxy)-N-(anthracen-9-ylmethyl)ethan-1-amine
AntPegOH and/or <b>2</b>	2-(2-(anthracen-9-ylmethylamino)ethoxy)ethanol
AntPegTerp and/or <b>L<sup>2</sup></b>	2-(2-([2,2':6',2''-terpyridin]-4'-yloxy)ethoxy)-N-(anthracen-9-ylmethyl)ethan-1-amine
ct-DNA	calf thymus DNA
CD	circular dichroism
cod	1,5-cyclooctadiene
DCM	dicloromethane
DMF	dimethylformamide
DMSO	dimethylsulfoxide
DNA	deoxyribonucleic acid
dNTPs	nucleoside triphosphates containing deoxyribose (d)
ESI-MS	electrospray ionisation mass spectrometry
FAM	fluorescein amidite
FRET	Fluorescence Resonance Energy Transfer
HPLC	high-pressure/high-performance liquid chromatography
LiCad	lithium cacodylate
LC-MS	liquid chromatography-mass spectrometry
NMR	Nuclear magnetic resonance
ORTEP	Oak Ridge thermal ellipsoid plot
PAGE	polyacrylamide gel electrophoresis
PSA	polymerase stop assay
[Pt(cod)Cl <sub>2</sub> ]	cis-dichlorido(1,5-cyclooctadiene)platinum(II)
QITMS	quadrupole ion trap mass spectrometry
RP-HPLC	reversed phase HPLC
SI	supplementary information
Taq	<i>Thermus aquaticus</i>
TAMRA	tetramethylrhodamine
TBE	tris/borate/EDTA
TLC	thin-layer chromatography

Tpy	terpyridine
TRIS	tris(hydroxymethyl)aminomethane
UV	ultraviolet
UV/Vis	ultraviolet-visible

#### Acknowledgements

This work was supported by COST action CM1105 (Functional metal complexes that bind to biomolecules), Fundação para a Ciência e a Tecnologia – FCT (projects PTDC/QUI-QUI/114139/2009, RECI/QEQ-QJN/0189/2012 and EXCL/QEQ-MED/0233/2012; grants SFRH/BPD/29564/2006 to SGama and FCT Investigator Grant to FMendes), EPSRC (EP/H005285/1), Collaborative Research Centre ChemBioSys (CRC 1127) funded by the Deutsche Forschungsgemeinschaft (DFG) and Newton Fellow of Royal Society. The authors would also like to thank Célia Fernandes for the Mass Spectrometry analysis, which was carried out on a QITMS instrument, acquired with the support of the Programa Nacional de Reequipamento Científico (Contract REDE/1503/REM/2005-ITN) of FCT and is part of RNEM-Rede Nacional de Espectrometria de Massa.

#### Appendix A. Supplementary data

Supplementary data to this article can be found online at <http://dx.doi.org/10.1016/j.jinorgbio.2016.04.002>.

#### References

- [1] S. Balasubramanian, Chemical biology on the genome, *Bioorg. Med. Chem.* 22 (2014) 4356–4370.
- [2] P. Murat, S. Balasubramanian, Existence and consequences of G-quadruplex structures in DNA, *Curr. Opin. Genet. Dev.* 25 (2014) 22–29.
- [3] N. Maizels, L.T. Gray, S.M. Rosenberg, The G4 genome, *PLoS Genet.* 9 (2013), e1003468.
- [4] S. Neidle, Human telomeric G-quadruplex: the current status of telomeric G-quadruplexes as therapeutic targets in human cancer, *FEBS J.* 277 (2010) 1118–1125.
- [5] B.P. Belotserkovskii, S.M. Mirkin, P.C. Hanawalt, DNA sequences that interfere with transcription: implications for genome function and stability, *Chem. Rev.* 113 (2013) 8620–8637.
- [6] S. Balasubramanian, L.H. Hurley, S. Neidle, Targeting G-quadruplexes in gene promoters: a novel anticancer strategy? *Nat. Rev. Drug Discov.* 10 (2011) 261–275.
- [7] G.W. Collie, G.N. Parkinson, The application of DNA and RNA G-quadruplexes to therapeutic medicines, *Chem. Soc. Rev.* 40 (2011) 5867–5892.
- [8] S. Neidle, G.N. Parkinson, The structure of telomeric DNA, *Curr. Opin. Struct. Biol.* 13 (2003) 275–283.
- [9] T. Simonsson, G-quadruplex DNA structures—variations on a theme, *Biol. Chem.* 382 (2001) 621–628.
- [10] A. Shivalingam, M. Angeles Izquierdo, A. Le Marois, A. Vysniauskas, K. Suhling, M.K. Kuimova, R. Vilar, The interactions between a small molecule and G-quadruplexes are visualized by fluorescence lifetime imaging microscopy, *Nat. Commun.* 6 (2015) 8178.
- [11] A. Henderson, Y. Wu, Y.C. Huang, E.A. Chavez, J. Platt, F.B. Johnson, R.M. Brosh, D. Sen, P.M. Lansdorp, Detection of G-quadruplex DNA in mammalian cells, *Nucleic Acids Res.* 42 (2014) 860–869.
- [12] G. Biffi, D. Tannahill, J. McCafferty, S. Balasubramanian, Quantitative visualization of DNA G-quadruplex structures in human cells, *Angew. Chem. Int. Ed. Eng.* 5 (2013) 182–186.
- [13] T.R. Cech, Life at the end of the Chromosome: Telomeres and Telomerase, *Angew. Chem. Int. Ed. Eng.* 39 (2000) 34–43.
- [14] A. de Cian, L. Lacroix, C. Douarre, N. Temime-Smaali, C. Trentesaux, J.-F. Riou, J.-L. Mergny, Targeting telomeres and telomerase, *Biochimie* 90 (2008) 131–155.
- [15] T.-M. Ou, Y.-J. Lu, C. Zhang, Z.-S. Huang, X.-D. Wang, J.-H. Tan, Y. Chen, D.-L. Ma, K.-Y. Wong, J.-C.-O. Tang, A.S.-C. Chan, L.-Q. Gu, Stabilization of G-quadruplex DNA and down-regulation of oncogene *c-myc* by quindoline derivatives, *J. Med. Chem.* 50 (2007) 1465–1474.
- [16] A. de Cian, P. Grellier, E. Mouray, D. Depoix, H. Bertrand, D. Monchaud, M.-P. Teulade-Fichou, J.-L. Mergny, P. Alberti, Plasmodium telomeric sequences: structure, stability and quadruplex targeting by small compounds, *ChemBioChem* 9 (2008) 2730–2739.
- [17] J.-L. Zhou, Y.-J. Lu, T.-M. Ou, J.-M. Zhou, Z.-S. Huang, X.-F. Zhu, C.-J. Du, X.-Z. Bu, L. Ma, L.-Q. Gu, Y.-M. Li, A.S.-C. Chan, Synthesis and evaluation of quindoline derivatives as G-quadruplex inducing and stabilizing ligands and potential inhibitors of telomerase, *J. Med. Chem.* 48 (2005) 7315–7321.
- [18] C.B. Harley, Telomerase and cancer therapeutics, *Nat. Rev. Cancer* 8 (2008) 167–179.
- [19] A. Siddiqui-Jain, C.L. Grand, D.J. Bearss, L.H. Hurley, Direct evidence for a G-quadruplex in a promoter region and its targeting with a small molecule to repress *c-MYC* transcription, *PNAS* 99 (2002) 11593–11598.

- [20] A. Rangan, O.Y. Fedoroff, L.H. Hurley, Induction of duplex to G-quadruplex transition in the *c-myc* promoter region by a small molecule, *J. Biol. Chem.* 276 (2001) 4640–4646.
- [21] A. Paul, S. Bhattacharya, Chemistry and biology of DNA-binding small molecules, *Curr. Sci.* 102 (2012) 212–231.
- [22] S.N. Georgiades, Nurul H. Abd Karim, K. Suntharalingam, R. Vilar, Interaction of metal complexes with G-quadruplex DNA, *Angew. Chem. Int. Ed. Engl.* 49 (2010) 4020–4034.
- [23] D. Monchaud, M.-P. Teulade-Fichou, A hitchhiker's guide to G-quadruplex ligands, *Org. Biomol. Chem.* 6 (2008) 627–636.
- [24] M.-P. Teulade-Fichou, C. Carrasco, L. Guittat, C. Bailly, P. Alberti, J.-L. Mergny, A. David, J.-M. Lehn, W. David Wilson, Selective recognition of G-quadruplex telomeric DNA by a bis(quinacridine) macrocycle, *J. Am. Chem. Soc.* 125 (2003) 4732–4740.
- [25] R. John Harrison, J. Cuesta, G. Chessari, M.A. Read, S.K. Basra, A.P. Reszka, J. Morrell, S.M. Gowan, C.M. Incles, F.A. Tanious, W. David Wilson, L.R. Kelland, S. Neidle, Tri-substituted acridine derivatives as potent and selective telomerase inhibitors, *J. Med. Chem.* 46 (2003) 4463–4476.
- [26] J.A. Schouten, S. Ladame, S.J. Mason, M.A. Cooper, S. Balasubramanian, G-quadruplex-specific peptide-hemicyanine ligands by partial combinatorial selection, *J. Am. Chem. Soc.* 125 (2003) 5594–5595.
- [27] A. Maraval, S. Franco, C. Vialas, G. Pratiel, M.A. Blasco, B. Meunier, Porphyrin-aminquinoline conjugates as telomerase inhibitors, *Org. Biomol. Chem.* 1 (2003) 921–927.
- [28] D. Sun, B. Thompson, B.E. Cathers, M. Salazar, S.M. Kerwin, J.O. Trent, T.C. Jenkins, S. Neidle, L.H. Hurley, Inhibition of human telomerase by a G-quadruplex-interactive compound, *J. Med. Chem.* 40 (1997) 2113–2116.
- [29] P.J. Perry, S.M. Gowan, A.P. Reszka, P. Polucci, T.C. Jenkins, L.R. Kelland, S. Neidle, 1,4- and 2,6-disubstituted amidoanthracene-9,10-dione derivatives as inhibitors of human telomerase, *J. Med. Chem.* 41 (1998) 3253–3260.
- [30] H. Han, D.R. Langley, A. Rangan, L.H. Hurley, Selective interactions of cationic porphyrins with G-quadruplex structures, *J. Am. Chem. Soc.* 123 (2001) 8902–8913.
- [31] N.H. Campbell, Nurul H. Abd Karim, G.N. Parkinson, M. Gunaratnam, V. Petrucci, A.K. Todd, R. Vilar, S. Neidle, Molecular basis of structure–activity relationships between salphen metal complexes and human telomeric DNA quadruplexes, *J. Med. Chem.* 55 (2012) 209–222.
- [32] J.E. Reed, A.A. Arnal, S. Neidle, R. Vilar, Stabilization of G-quadruplex DNA and inhibition of telomerase activity by square-planar nickel(II) complexes, *J. Am. Chem. Soc.* 128 (2006) 5992–5993.
- [33] A. Arola-Arnal, J. Benet-Buchholz, S. Neidle, R. Vilar, Effects of metal coordination geometry on stabilization of human telomeric quadruplex DNA by square-planar and square-pyramidal metal complexes, *Inorg. Chem.* 47 (2008) 11910–11919.
- [34] H. Bertrand, D. Monchaud, A. de Cian, R. Guillot, J.-L. Mergny, M.-P. Teulade-Fichou, The importance of metal geometry in the recognition of G-quadruplex-DNA by metal-terpyridine complexes, *Org. Biomol. Chem.* 5 (2007) 2555–2559.
- [35] A. Granzhan, D. Monchaud, N. Saettel, A. Guedin, J.-L. Mergny, M.-P. Teulade-Fichou, "One ring to bind them all"-part I: the efficiency of the macrocyclic scaffold for g-quadruplex DNA recognition, *J. Nucleic Acids* (2010), 525862 (19 pages).
- [36] V.S. Stafford, K. Suntharalingam, A. Shivalingam, Andrew J.P. White, D.J. Mann, R. Vilar, Syntheses of polypyridyl metal complexes and studies of their interaction with quadruplex DNA, *J. Chem. Soc. Dalton Trans.* 44 (2015) 3686–3700.
- [37] H. Bertrand, S. Bombard, D. Monchaud, E. Talbot, A. Guedin, J.-L. Mergny, R. Grunert, P.J. Bednarski, M.-P. Teulade-Fichou, Exclusive platination of loop adenines in the human telomeric G-quadruplex, *Org. Biomol. Chem.* 7 (2009) 2864–2871.
- [38] E. Largy, F. Hamon, F. Rosu, V. Gabelica, E. de Pauw, A. Guedin, J.-L. Mergny, M.-P. Teulade-Fichou, Tridentate *N*-donor palladium(II) complexes as efficient coordinating quadruplex DNA binders, *Chemistry* 17 (2011) 13274–13283.
- [39] K. Suntharalingam, Andrew J.P. White, R. Vilar, Synthesis, structural characterization, and quadruplex DNA binding studies of platinum(II)-terpyridine complexes, *Inorg. Chem.* 48 (2009) 9427–9435.
- [40] K. Suntharalingam, Andrew J.P. White, R. Vilar, Two metals are better than one: investigations on the interactions between dinuclear metal complexes and quadruplex DNA, *Inorg. Chem.* 49 (2010) 8371–8380.
- [41] SMART, SAINT and SADABS, Bruker AXS Inc., Madison, Wisconsin, USA, 2005.
- [42] S.G.M. Sheldrick, SADABS, Bruker AXS Inc., Madison, Wisconsin, USA, 2004.
- [43] A. Altomare, M. C. Burla, M. Camalli, G. L. Casciaro, C. Giacovazzo, A. Guagliardi, A. G. G. Moliterni, G. Polidori, R. Spagna, *J. Appl. Cryst.* (115).
- [44] G.M. Sheldrick, SHELX97 - Programs for Crystal Structure Analysis (Release 97–2), Tammanstrasse 4, D-3400 Göttingen, Germany, 2008.
- [45] L. Farrugia, WinGX and ORTEP for Windows: an update, *J. Appl. Crystallogr.* 45 (2012) 849–854.
- [46] L. Farrugia, ORTEP-3 for Windows - a version of ORTEP-III with a Graphical User Interface (GUI), *J. Appl. Crystallogr.* 30 (1997) 565.
- [47] J.L. Bresloff, D.M. Crothers, Equilibrium studies of ethidium-polynucleotide interactions, *Biochemistry* 20 (1981) 3547–3553.
- [48] J.D. McGhee, Peter H. von Hippel, Theoretical aspects of DNA-protein interactions: co-operative and non-co-operative binding of large ligands to a one-dimensional homogeneous lattice, *J. Mol. Biol.* 86 (1974) 469–489.
- [49] W. Henke, S. Kremer, D. Reinen, Copper(2+) in five-coordination: a case of a pseudo-Jahn-Teller effect. 1. Structure and spectroscopy of the compounds Cu(terpy)X<sub>2</sub>.nH<sub>2</sub>O, *Inorg. Chem.* 22 (1983) 2858–2863.
- [50] J.R. Shaple (Ed.), *Inorganic Synthesis: Cationic Pt(II) Complexes of Tridentate Amine Ligands*, Wiley, United States, 2004.
- [51] J.X. McDermott, J.F. White, G.M. Whitesides, Thermal decomposition of bis(phosphine)platinum(II) metallocycles, *J. Am. Chem. Soc.* 98 (1976) 6521–6528.
- [52] A.K. Fazlur-Rahman, J.G. Verkade, Reactions of chloro(diethylenetriamine)platinum(1+) chloride and chloro(terpyridine)platinum(1+) chloride with thiols, thioethers, and dialkyl disulfides: a platinum-195 NMR study, *Inorg. Chem.* 31 (1992) 2064–2069.
- [53] A. Bahreman, J.-A. Cuello-Garibo, S. Bonnet, Yellow-light sensitization of a ligand photosubstitution reaction in a ruthenium polypyridyl complex covalently bound to a rhodamine dye, *J. Chem. Soc. Dalton Trans.* 43 (2014) 4494–4505.
- [54] A. Rodger, S. Taylor, G. Adlam, I.S. Blagbrough, I.S. Haworth, Multiple DNA binding modes of anthracene-9-carbonyl-N1-spermine, *Bioorg. Med. Chem.* 3 (1995) 861–872.
- [55] T.P. Wunz, M.T. Craven, M.D. Karol, G. Craig Hill, W.A. Remers, DNA binding by antitumor anthracene derivatives, *J. Med. Chem.* 33 (1990) 1549–1553.
- [56] L. Ren, A. Zhang, J. Huang, P. Wang, X. Weng, L. Zhang, F. Liang, Z. Tan, X. Zhou, Quaternary ammonium zinc phthalocyanine: inhibiting telomerase by stabilizing G quadruplexes and inducing G-quadruplex structure transition and formation, *ChemBiochem* 8 (2007) 775–780.